JOURNAL OF AGRICULTURAL AND FOOD CHEMISTRY

Thermospectroscopic Study of the Adsorption Mechanism of the Hydroxamic Siderophore Ferrioxamine B by Calcium Montmorillonite

HAGAR SIEBNER-FREIBACH,† YITZHAK HADAR,‡ SHMUEL YARIV,§ ISAAK LAPIDES,§ AND YONA CHEN*,†

Departments of Soil and Water Sciences and of Microbiology and Plant Pathology, Faculty of Agricultural, Food and Environmental Quality Sciences, The Hebrew University of Jerusalem, P.O. Box 12, Rehovot 76100, and Department of Inorganic Chemistry, The Hebrew University of Jerusalem, Jerusalem 91904, Israel

The behavior of iron-chelating agents in soils is highly affected by interactions with the solid phase. Still this aspect is frequently ignored. In this research the adsorption of the siderophore ferrioxamine B by Ca-montmorillonite, as a free ligand (desferrioxamine B, DFOB) and as a complex with Fe^{3+} (ferrioxamine B, FOB), was studied, using thermo X-ray diffraction (thermo-XRD) in the temperature range 25−360 °C and thermo-FTIR spectroscopy in the temperature range 25−170 °C. The effect of pH (4−7.5) on the adsorption was examined. Extensive use of curve-fitting analysis was required due to significant overlapping of the characteristic absorption bands of the various functional groups. Thermo-XRD analysis showed that both DFOB and FOB penetrated into the interlayer space of Ca-montmorillonite. FTIR results indicated strong interactions of DFOB within the interlayer, which involved all functional groups (NH_3^+, secondary amide groups, and hydroxamate groups). In contrast, the folded Fe complex of FOB retained its molecular configuration upon adsorption, and the basal spacing of the clay increased correspondingly. FOB interacted in the interlayer space of the clay, mainly through the NH of the secondary amide groups and NH_3^+, while the functional groups bound to the central Fe cation remained unchanged. The suspension pH had no significant effect on both DFOB and FOB adsorption at the examined range. Adsorption protected the adsorbates from thermal degradation compared to the nonadsorbed samples up to 105 °C. At 170 °C both DFOB and FOB were already partially degraded, but to a lesser extent than the nonadsorbed samples. Degradation of the molecules occurred mainly through the hydroxamic groups, which constitute the Fe-chelating center in the hydroxamic siderophore.

KEYWORDS: Adsorption; Ca-montmorillonite; ferrioxamine B; FTIR spectroscopy; X-ray; siderophore

INTRODUCTION

Iron is a vital nutrient for all living organisms. Despite its abundance in soils, plants growing in neutral to alkaline soils are often subjected to Fe deficiency due to its low solubility under the pH and redox conditions prevailing in these environments (*1*, *2*). However, the Fe concentration in soil solutions is often higher than that expected from chemical equilibrium equations of soil Fe minerals. This enhancement is partially ascribed to the presence of organic molecules exhibiting various extents of Fe-chelation abilities (*3*). A unique group of these organic molecules are microbial siderophores, which are low molecular weight chelates secreted by microorganisms under Fe deficiency aimed to scavenge Fe from its environment. Fe−siderophore complexes are then efficiently taken up by their producer, or by other microorganisms (*4*). Siderophore concentrations, high enough to positively affect plant nutrition, were found in soil extracts (*5*−*8*).

The microbial siderophore ferrioxamine B was chosen in this study because of its extensive use in siderophore research and its presence in soils. It is produced by *Streptomyces* and *Nocardia* bacteria (*9*) and belongs to the group of hydroxamate siderophores. Iron carried by ferrioxamine B has been found to be an efficient source of Fe for many microorganisms (*4*), as well as for a variety of plants (see, e.g., refs *10*−*14*).

The ferrioxamine molecule is a hexadentate ligand consisting of three bidentate hydroxamic groups (**Figure 1a**). The residual chain includes two secondary amide groups and an aliphatic chain. The saturated amine group on one edge of the linear molecule gives the molecule a positive charge in acid to slightly

* To whom correspondence should be addressed. Phone: +972-8-9489234. Fax: +972-8-9468565. E-mail: yonachen@agri.huji.ac.il.
† Department of Soil and Water Sciences.
‡ Department of Microbiology and Plant Pathology.
§ Department of Inorganic Chemistry.

10.1021/jf051924e CCC: $33.50
Published on Web 01/20/2006

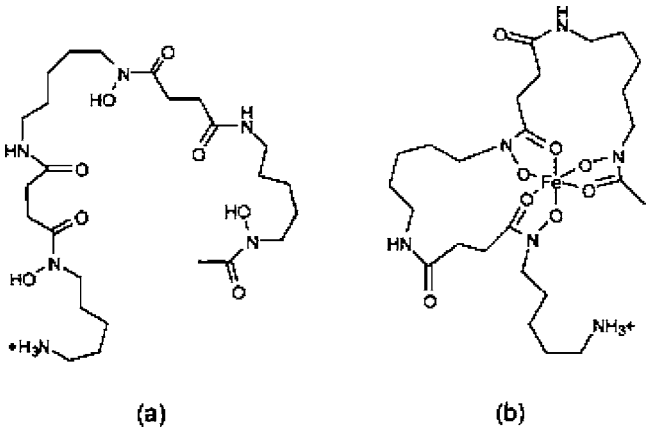

Figure 1. Schematic diagrams of (**a**) DFOB (desferrioxamine B, the free ligand of the siderophore ferrioxamine B) and (**b**) FOB (the ferric complex of DFOB).

alkaline solutions (*15*). Upon Fe^{3+} chelation, oxygen atoms of the hydroxamate groups bind to the Fe (**Figure 1b**), the three hydroxyls are deprotonated, and three identical asymmetrical chelation rings are formed, creating a distorted octahedron centered by Fe. The open chain, ending with the NH_3^+, has been found to point away from the Fe center (*16*). The Fe complex (FOB) obtains a wide, fairly flat configuration, total thickness 0.55 nm (*16*), presenting a rather hydrophobic face, in contrast with the linear open chain with exposed active sites of the free ligand (desferrioxamine B, DFOB). The methylsulfonate salt of desferrioxamine B is marketed under the name Desferal as a therapeutic agent.

Due to the high prevalence of clays in soils, adsorption to clay is of great importance to the reactivity of siderophores and their distribution in soils. In an earlier study we reported on a significant adsorption of this siderophore to montmorillonite (*17*). Experiments with plants proved that they are able to use these adsorbed siderophores as an Fe source (*14*). The clay fraction of soils in arid and semiarid regions, in which Fe deficiency is common, usually contains high levels of montmorillonite as well as Ca^{2+} ions. Therefore, we chose to focus our study on the adsorption of both the free ligand (DFOB) and its Fe complex (FOB) to a monoionic Ca-montmorillonite.

Thermo-FTIR spectroscopy is an attractive technique for the study of the interaction between organic molecules and clays and the fine structure of the organoclay complexes (*18*). A point of concern however is the significant overlapping of characteristic absorption bands, which takes place in spectra measured for both DFOB and FOB. A comprehensive interpretation of characteristic bands in these spectra, using a curve-fitting technique, was presented in a previous paper of our group (*19*). On the basis of these data, a detailed thermo-FTIR spectroscopy analysis of the adsorbed siderophore was performed in the current study.

The interlayer space of montmorillonite constitutes a special environment, which could affect the adsorption mechanism as well as availability of the siderophore to plants and microorganisms. Thus, it is highly important to determine whether the adsorption of the siderophore takes place within the interlayer space. A definite answer can be obtained using thermo X-ray diffraction (thermo-XRD) analysis (*20*), which was applied as well in this study.

The characterization of the adsorption mechanism of both forms of the siderophore (DFOB and FOB) by Ca-montmorillonite could have significant implications concerning its function in agriculture. It may also have an ecological significance since this siderophore is produced by soil-originated bacteria. The adsorption of the siderophore to soil components could affect significantly the competitive ability of its producer toward other microorganisms, as well as its distribution in different soil types. To date, no detailed research has been conducted on the adsorption mechanism of siderophores to clays and the differences in adsorption of a chelating agent and its Fe complex. We therefore conducted this study aiming to elaborate on mechanisms of these interactions.

MATERIALS AND METHODS

Materials. The methylsulfonate salt of the desferric form of the microbial siderophore (DFOB) was purchased as the medical reagent Desferal from Ciba-Geigy Ltd. (Basel, Switzerland). The product was dissolved in distilled water. Its complex with Fe (FOB) was prepared by adding $FeCl_3$ to a solution of the free ligand at a 10% excess of Fe over the ligand, then centrifuged at 106000*g*, and filtered through a 0.1 μm filter to remove Fe colloids. Solutions of both DFOB and FOB were prepared at three pH values (4.0, 6.0, and 7.5). The pH was adjusted to the desired level with $HClO_4$ and KOH.

The clay fraction (<2 μm) of the mineral montmorillonite (Wyoming bentonite) was separated from the bulk, using sedimentation. To prepare monoionic Ca^{2+}-montmorillonite, the clay fraction was saturated with Ca^{2+} by washing it three consecutive times with an excess of 1.0 M $CaCl_2$ solution and then with distilled water until the suspension was free of chloride. The clay was separated from the suspension by centrifugation, then freeze-dried, and ground.

Adsorption of the Siderophore by Ca-Montmorillonite. Adsorption of DFOB and FOB by Ca-montmorillonite was performed at three pH levels: 4.0, 6.0, and 7.5. The clay suspensions were prepared with water and $KClO_4$ to achieve a final clay concentration of 5 g·L^{-1} and an ionic strength of 0.01 M in the final reaction flask. The pH was adjusted using KOH and $HClO_4$. The clay suspensions were mixed with DFOB or FOB solutions in polypropylene centrifuge tubes. The final concentration of DFOB and FOB in the reaction tubes was 1.0 mM. This concentration was chosen because it results in an adsorption level located within the linear part of the adsorption isotherms (*17*) to avoid multilayer adsorption. For comparison, unloaded Ca-montmorillonite samples contained clay suspensions with $KClO_4$ at the same pH levels. The suspensions in the centrifuge tubes were brought to a final volume of 10 mL with distilled water. The tubes were shaken for 3 days (time was chosen according to previously measured kinetic studies; *17*), at 25 °C, and then centrifuged at 25 °C and 40000*g* for 10 min. The precipitates were washed and centrifuged repeatedly with distilled water until no traces of DFOB or FOB were detected in the supernatants. Then they were freeze-dried, ground, and kept in a desiccator.

The supernatant was filtered through a 0.45 μm filter of cellulose acetate. The concentration of the nonsorbed FOB in the supernatant solution was measured using a Hewlett-Packard 8452A diode array spectrophotometer at 428 nm. To facilitate measurements of the free ligand DFOB, Fe was added to the filtrate as $FeCl_3$ and then a HEPES buffer solution was added (0.2 M, pH 7.5). After 1 h of equilibration at each stage, the solutions were filtered through 0.45 μm filters to remove the excess suspended Fe. Then the concentration of the formed ferric complex (FOB) was measured. Adsorption was calculated by the difference between the initial and final concentrations in the filtrates. The adsorbed amounts by unloaded, DFOB-loaded, and FOB-loaded Ca-montmorillonite were 0, 0.17, and 0.16 mmol·g^{-1}, respectively. Adsorption to all experimental containers and filters was tested and found negligible.

Thermo-XRD Analysis. Oriented specimens of unloaded, DFOB-loaded, and FOB-loaded Ca-montmorillonite were obtained by air-drying 1 mL of the appropriate suspension (1%) on a glass slide. Each sample was heated for 3 h at each temperature: 120, 250, and 360 °C. Patterns of X-ray diffraction of these samples were recorded at room temperature, before the thermal treatment and immediately after it, using a Philips automatic diffractometer (PW 1710) with a Cu anode tube.

Thermo-FTIR Spectroscopy Analysis. Air-dried samples of unloaded, DFOB-loaded, and FOB-loaded Ca-montmorillonite at the

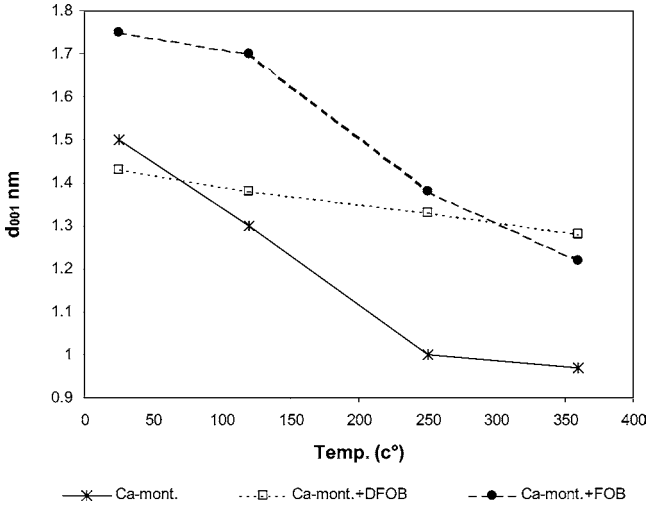

Figure 2. Effect of thermal treatments on the basal spacing of unloaded Ca-montmorillonite compared with DFOB- or FOB-loaded Ca-montmorillonite.

different pH levels, with KBr (for IR spectroscopy) at 25 °C, were pressed into 100 mg disks. Samples contained 1 mg of adsorbed DFOB or FOB (calculated according to the measured adsorption). Disks were reground gently and repressed. This procedure was applied to homogeneously scatter the examined substances in the disk. Samples then were gradually heated overnight to 60, 105, and 170 °C. After the thermal treatment the disk became opaque, and it was thus repressed (without regrinding) to restore transparency. The infrared spectra were recorded using a Nicolet Magna-IR model 550, at a resolution of 4 cm^{-1}.

Curve-Fitting. The curve-fitting process was performed following the guidelines described in detail in our previous paper (*19*). Briefly, curve-fitting was performed using the data-processing software GRAMS/AI of Thermo Galactic. It uses the Levenberg−Marquardt algorithm when the gradient is far from the minimum; then it switches to the Hessian-matrix methods to determine the best possible solution when the algorithm reaches a minimum value of χ^2. Baseline corrections and analysis were performed over spectral ranges which were as restricted as possible. Since the Lorentzian line shape provided good results, we chose to use it in the curve-fitting process. The root mean squared (RMS) noise was graphically estimated over a narrow examined range (otherwise the Savitzki−Golay smoothing algorithm resulted in artificially high levels of reduced χ^2 for DFOB and FOB spectra). A value 2 orders of magnitude lower was then manually inserted to avoid possible overestimation of the RMS noise. Solutions were accepted only when they converged, and good and highly reproducible χ^2 values were obtained. Bands of the siderophore in a frequency range lower than 1240 cm^{-1} were practically not applicable for the curve-fitting analysis due to high absorption bands of the clay within this range.

RESULTS

Thermo-XRD. Changes in the basal spacing following heating from 25 °C to 120, 250, and 360 °C are summarized in **Figure 2**. The initial basal spacings measured for unloaded Ca-montmorillonite blank and Ca-montmorillonite loaded with DFOB or FOB were 1.50, 1.43, and 1.75 nm, respectively. Upon heating of the unloaded Ca-montmorillonite sample, this spacing collapsed to 0.97 nm. In contrast, in samples containing the adsorbed siderophore (DFOB or FOB), the basal spacing, following all thermal treatments, was maintained at values higher than 1.25 nm.

FTIR Spectra. At the high frequency range, absorption bands of the clay-adsorbed water partially overlapped the bands of the siderophore. Curve-fitting analysis of this range enabled the discrimination of bands.

The spectra, resulting from the 60 °C thermal treatment, were not significantly different from those of 25 °C, and therefore, they are not shown in the figures. Data obtained at different thermal treatments and analyzed by the curve-fitting technique are summarized for DFOB and FOB spectra, at pH 7.5, in **Tables 1** and **2**, respectively. The tables include band assignments, frequencies of the maxima, relative band intensities, and band shapes.

FTIR Spectra of Adsorbed DFOB. Adsorption of DFOB by Ca-montmorillonite strongly affected its FTIR spectrum (**Figure 3**, **Table 1**). New absorption bands appeared in the spectra of adsorbed DFOB in the range of 3250−3170 cm^{-1}. Fitting of this range resulted in two bands at 3236 and 3193 cm^{-1} at 25 °C (**Figure 4**, **Table 1**). However, while the location of these bands was very stable and reproducible, the curve-fitting analysis did not give an unequivocal result regarding their size. Some effects of the 105 °C treatment on adsorbed DFOB compared to the free (nonadsorbed) form are shown in **Figure 5** (see the Discussion).

The spectra of adsorbed DFOB did not differ significantly at different pH values (**Figure 6**). Differences demonstrated at the higher frequency range were related solely to hydration water (since these spectra are given after subtraction of the unloaded Ca-montmorillonite spectrum, this range is affected by the water content of the clay as well).

FTIR Spectra of Adsorbed FOB. The spectra of FOB did not change significantly following adsorption (**Figure 7**, **Table 2**). The enhanced broadness and shape of the absorption band at 3250−3170 cm^{-1} assigned to NH_3^+ implied the existence of two bands in this range, similar to those of DFOB. In contrast to that of the latter, the location of these bands could not be unequivocally determined by the curve-fitting analysis. Thus, the best guess, which provided two bands at 3228 and 3183 cm^{-1}, was chosen. In the lower frequency range, the effects of adsorption on the spectrum of FOB were minor, excluding the appearance of a series of new small bands at the range of 1542−1489 cm^{-1} (**Table 2**). These bands partially disappeared after heating to 105 °C.

The spectrum of FOB did not vary significantly at different pH levels (**Figure 8**). Changes in the higher range, observed at different pH levels, were related to the hydration water, as was mentioned for DFOB.

Thermal Treatment at 170 °C. The resemblance of the spectra of the adsorbed DFOB to those of adsorbed FOB after heating of the sample to 170 °C is shown in **Figure 9**. A similar resemblance was found for the spectra of the free compounds following this treatment (*19*). However, changes observed in the spectra of both adsorbates (DFOB and FOB) upon heating were smaller than those observed for the free (not adsorbed) compounds. The strong band at 1699 cm^{-1} and medium band at 1666 cm^{-1} exhibited in the spectra of both free DFOB and FOB after the 170 °C treatment did not appear in this case. The absorption intensity at the range of 1500−1350 cm^{-1} decreased. The absorption band at 1400 cm^{-1} was not enhanced as opposed to the effect observed in the spectrum of the free molecule, following the same treatment.

DISCUSSION

X-ray Diffractograms. The thermo X-ray diffraction analysis (**Figure 2**) showed that both DFOB and FOB penetrated into the interlayer space. Due to the thermal treatment at 360 °C, the organic matter within the interlayer space was converted into a charcoal, thus preventing the collapse of the basal spacing (*20*). Indeed, while the basal spacing of the unloaded Ca-

Table 1. Maxima of the Absorption Bands[a] in the Curve-Fitted Infrared Spectra of Adsorbed DFOB Compared with Those of the Free (Nonsorbed) DFOB,[b] pH 7.5

band assignment	frequency (cm^{-1})			
	free, 25 °C[b]	free, 105 °C[b]	adsorbed, 25 °C	adsorbed, 105 °C
HOH stretch	3464 w, vbr			3448 w
			3423 s, br	3423 w
			3359 s, br	3397 w
				3347 w
N–H stretch, secondary amide (hydrated)	3313 vs, sp	3317 s, sp	3285 s	3288 s
N–H stretch, secondary amide (anhydrous)		3266 m, br		
NH_3^+–H_2O–clay			3236 m	3242 m
NH_3^+–clay			3193 m	3192 w
O–H stretch	3149 s, br	3160 s, vbr	3120 m, vbr	3114 s, vbr
C–N–H overtone	3096 w	3090 m		
NH_3^+ asymmetric stretch	3013 m	3015 m	3032 w, vbr	3033 m, br
				2993 w
CH_3 asymmetric stretch	2967 w, sp	2966 m, sp	2960 w	2963 m
CH_2 asymmetric stretch	2933 vs, sp	2934 s, sp	2936 vs	2941 vs
NH_3^+ symmetric stretch	2901 m	2902 s, br	2963 w, br	2907 vw
CH_3 symmetric stretch	2875 vw, sp	2868 w	2877 w	2879 m
CH_2 symmetric stretch	2856 m, sp	2856 m, sp	2863 m	2864 m
NH_3^+ overtones and combination tones	2821 vw	2821 w, br	2810 vw, br	2825 w
	2790 m, vbr	2763	2756 vw, br	2763 w, vbr
	2652 w	2657	2635 vw, br	2633 vw
	2535 w	2544		2533 vw
product of decomposition	1697 vvw	1700 m	1717 vvw, vbr	
C═O stretch, out of phase (secondary amide)			1665 w	1664 w
C═O stretch, in phase (secondary amide)	1651 m	1649 s	1650 s	1650 m
HOH deformation	1634 s	1635 vw	1635 s	1636 m
C═O stretch (hydroxamate)	1624 vs	1623 vs	1619 s	1620 s
NH_3^+ asymmetric deformation	1608 m, br	1605 vw, br	1606 m	1606 m
C–N–H (secondary amide)	1571 m	1570 m		
C–N–H (secondary amide)	1564 m	1561 m	1557 w	1557 w
NH_3^+ symmetric deformation	1551 m, br	1547 m	1542 w	1542 w
	1529 vw, vbr	1534 w, vbr	1523 vw, br	1525 vw
			1507 vw	1507 vw
	1488 vw, vbr		1491 vw, br	1491 vw, br
			1473 w	1473 w
CH_2	1463 w, br		1465 vw	1466 vw
CH_3	1461 m	1459 m	1457 w	1458 w
C–H vibrations; the exact location derives from	1453 w		1447 vw	1441 w, br
the adjacency of different functional groups	1436 w	1437 w	1435 vw, br	
	1424 w	1425 w	1422 vw	1428 w
	1416 w	1416 w		1419 vw
		1404 w		
O–H deformation	1397 m	1397 w, sp		
	1384 vw			
CH_3	1373 w	1373 w	1376 w, vbr	1371 w, vbr
C–N stretch, N–H bend (secondary amide)	1271	1271	1261	1263
	1254	1254		

[a] The relative band height (s, strong; m, medium; w, weak; v, very) and shape (sp, sharp; br, broad) are described. [b] Reference *19*.

montmorillonite decreased to 0.97 nm after heating to 360 °C, that of DFOB- and FOB-loaded Ca-montmorillonite decreased to 1.28 and 1.22 nm only, respectively. At 25 °C the folded FOB molecule caused an enlargement of the basal spacing from 1.50 nm (unloaded Ca-montmorillonite) to 1.75 nm. Dhungana et al. (*16*) measured a total thickness of 0.55 nm for the FOB molecule. If the molecule was lying with its plane parallel to the montmorillonite layers, one would expect a basal spacing of 1.50−1.55 nm. The measured basal spacing of 1.75 nm, which decreased to 1.70 nm after the dehydration of the clay at 120 °C (**Figure 2**), suggests that the adsorbed FOB was lying slightly tilted within the clay layers.

The exchange of the hydrophilic Ca^{2+} by the DFOB cation caused a decrease of the basal spacing of Ca-montmorillonite from 1.50 nm (unloaded Ca-montmorillonite) to 1.42 nm, indicating a water loss. This observation supports the thermo-XRD conclusion, indicating the presence of the DFOB molecule within the interlayer space. After thermal dehydration at 120 °C the basal spacing decreased to 1.38 nm. Since the van der Waals diameter of C is 0.35 nm, this basal spacing suggests that the adsorbed DFOB formed a monolayer, lying almost parallel to the silicate layers (*21*, *20*).

FTIR Spectra. Assignment of bands observed in the spectra of free DFOB and FOB, to the various functional groups, was analyzed in detail in a previous paper (*19*). The data are used in the following discussion to assess the involvement of each functional group in the adsorption process (**Tables 1** and **2**, respectively).

Adsorbed DFOB. In general, the intensity of the bands decreased significantly upon adsorption (note the reduced scale in adsorbed DFOB, **Figure 3a,b**, compared to that of free DFOB in **Figure 3c,d**), implying significant fixation of functional groups due to adsorption. The sharpness of the bands also decreased, implying that hydrogen bonds are involved in the adsorption. These bonds could be produced either by accepting protons from Bronsted acidic sites, such as interlayer water molecules, or by donating protons to basic sites, such as atoms of the oxygen planes of the clay, or basic water molecules (*18*).

Table 2. Maxima of Absorption Bands[a] in the Curve-Fitted Infrared Spectra of Adsorbed FOB Compared with Those of the Free (Nonsorbed) FOB,[b] pH 7.5

band assignment	frequency (cm^{-1})			
	free, 25 °C[b]	free, 105 °C[b]	adsorbed, 25 °C	adsorbed, 105 °C
HOH stretch	3619		3484 s, br	
	3587		3425 s, br	
	3554		3419 m, br	3418 s
	3518		3372 s	3369 w
	3479		3340 m	3334 m
	3435			
	3381			
N–H stretch (secondary amide)	3269 vs, br	3274 s, br	3283 s, br	3288 s
NH_3^+–H_2O–clay			3228 m	3250 m
NH_3^+–clay			3183 m	3198 m, br
	3159 vw, vbr			
C–N–H overtone	3084 m	3071 s, br	3105 m	3100 m
NH_3^+ asymmetric stretch	3012 m	3013 w	3038 m, vbr	3029 m, br
				2991 w
CH_3 asymmetric stretch	2951 vw	2986 w	2960 w	2963 m
CH_2 asymmetric stretch	2932 vs, sp	2933 vs,	2939 s	2938 vs, sp
NH_3^+ symmetric stretch	2947 m, br	2939 m	2976 w, vbr	2906 w
CH_3 symmetric stretch	2872 w, sp	2871 w	2873 w	2875 m
CH_2 symmetric stretch	2858 m, sp	2859 m	2862 w	2862 m, sp
NH_3^+ overtones and combination tones	2817 w	2815 m, br	2813 vw	2813 w, br
	2752 w	2745 w, br	2760 vw	2745 vw
	2653 w	2646 w, br		
	2550 w	2545 w, br		
product of decomposition	1708 vw, vvbr		1716 w, vbr	1717 vw, vbr
C═O stretch, out of phase (secondary amide)	1665 m	1669 m	1666 m	1668 w
C═O stretch, in phase (secondary amide)	1650 s	1650 m	1650 s	1650 s
HOH deformation	1638 m	1636 w	1636 s	1635 s
	1625 w		1623 m	
C═O stretch, out of phase (hydroxamate)	1586 m	1586 m	1587 m	1589 m
C═O stretch, in phase (hydroxamate)	1573 vs	1573 s	1576 s	1578 m
			1559 vw	
NH_3^+ symmetric deformation	1550 m, br	1545 m, br	1548 m, br	1561 m, br
			1542 vw	1542 vw
			1522 vw	
	1512 vvw		1507 vw	1507 vw
			1489 vw	
CH_2	1471 w	1472 m	1471 m	1469 m
			1464 w	
CH_3	1459 s	1461 m	1458 m, sp	1458 vw
C–H vibrations; the exact location derives from	1449 w	1450 w	1447 m	1447 m
the adjacency of different functional groups	1436 w	1438 w	1437 w	1437 vw
	1421 w	1421 m, br	1422 m	1421 w
	1411 vw		1402 vvw, vvbr	
	1373	1373	1373	1373
CH_3	1360	1363	1363	1363
C–N stretch, N–H bend (secondary amide)	1261	1260	1263	1264

[a] The relative band height (s, strong; m, medium; w, weak; v, very) and shape (sp, sharp; br, broad) are described. [b] Reference *19*.

(i) Secondary Amide Groups. A significant decrease of the NH stretching frequency from 3313 to 3285 cm^{-1} following the adsorption (**Figure 3a** compared with **Figure 3c**, **Table 1**) is an indication of significant hydrogen bonding. The location of this band did not change at 105 °C, implying that dehydration of this group was not involved in this process. Other characteristic absorption bands of this group showed the same effect (**Figure 3b**, **Table 1**): The two bands at 1571 and 1564 cm^{-1}, related to the amide II band (C−N−H group), merged into one band at 1557 cm^{-1}, and the couple at 1271 and 1254 cm^{-1} merged into one band at 1261 cm^{-1}. This is in contrast to previous studies that showed a split in the amide II bands due to adsorption (e.g., for alachlor; *22*), which was attributed to the formation of different types of hydrogen bonds. The spectrum of the adsorbed DFOB, showing only one amide II band, implied a specific conformation of the DFOB at the interlayer of the clay, involving binding through the NH of secondary amides. Due to the rigid structure formed by that specific conformation, the C═O vibration splits into two bands in the spectrum of adsorbed DFOB; the first band appeared at 1665 cm^{-1}, representing out-of-phase vibration of the C═O of the fixated secondary amide. The in-phase vibration of this group remained at 1650 cm^{-1}, indicating that no significant change occurred in its immediate environment. The changes occurred in the spectrum of the secondary amide group due to adsorption, giving it the same characteristics as that of a fixed stable structure, which appeared for this group in the spectrum of free (nonadsorbed) DFOB following Fe complexation (*19*).

Bands of the secondary amide at about 3280, 1560, and 1650 cm^{-1} were maintained after heating to 170 °C (**Figure 9**). The persistence of this group in the adsorbed form at 170 °C is in contrast with that found for the free (nonadsorbed) ligand, which disappeared completely under similar conditions (*19*). This observation implied a protective effect of adsorption against the thermal degradation of this group.

(ii) Hydroxamate Groups. Following adsorption by Ca-montmorillonite, the frequency of the stretching vibration of the hydroxamic C═O shifted slightly toward a lower value

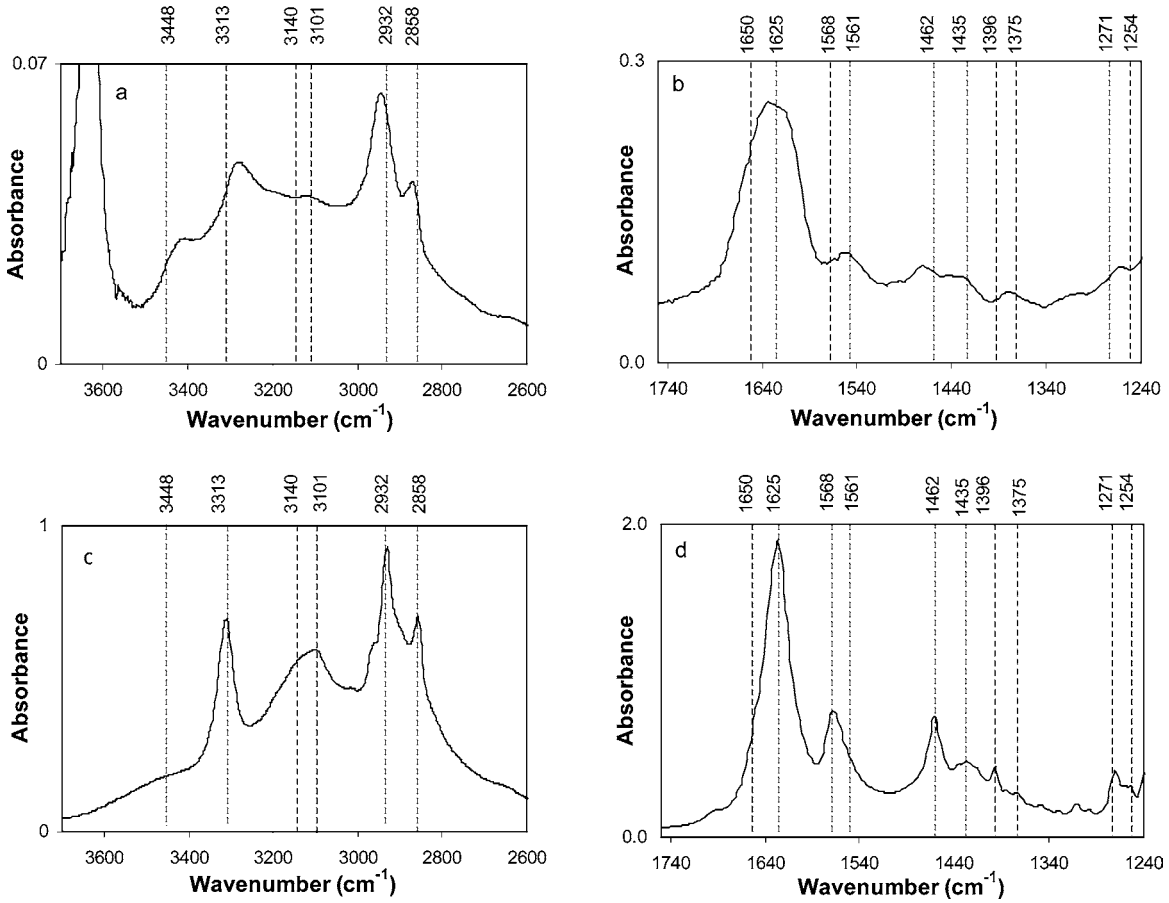

Figure 3. Effects of adsorption on the infrared spectra of DFOB (1 mg, 25 °C, pH 7.5), after subtraction of the unloaded Ca-montmorillonite spectrum: (**a**) adsorbed DFOB spectrum in the range of 3700–2600 cm^{-1}; (**b**) adsorbed DFOB spectrum in the range of 1750–1240 cm^{-1}; (**c**) free DFOB spectrum in the range of 3700–2600 cm^{-1}; (**d**) free DFOB spectrum in the range of 1750–1240 cm^{-1}.

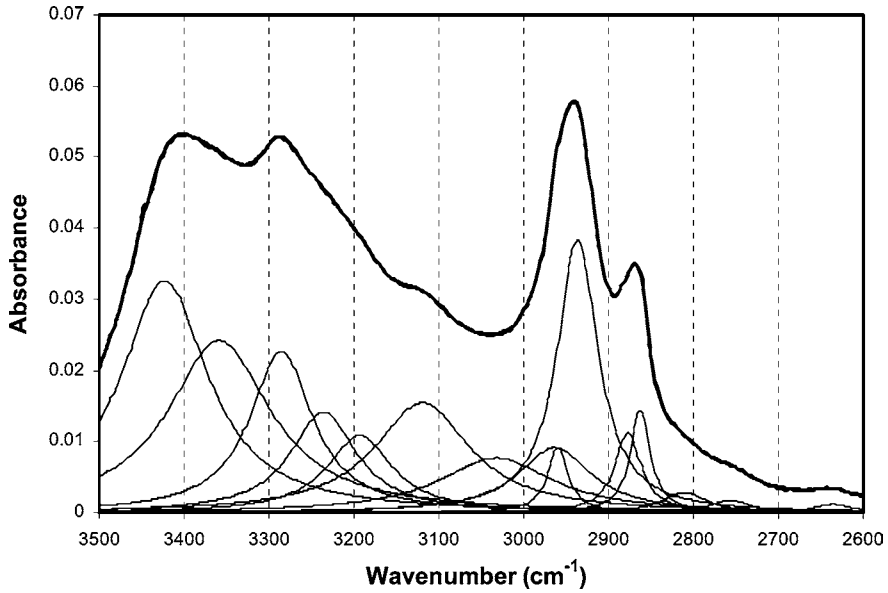

Figure 4. Curve-fitted spectra of adsorbed DFOB recorded in the range of 3500–2600 cm^{-1}. The spectrum was recorded on a KBr disk (25 °C, pH 7.5). Bold lines represent the measured spectrum and fitted line, which are overlapping. Gray lines represent the spectra assembling the fitted line as it was analyzed using GRAMS/AI software produced by Thermo Galactic. Peak values and the appropriate assignments are detailed in **Table 1**.

(**Figure 3b**, **Table 1**). The C═O group could be either bound to the exchangeable cation through a water bridge or directly coordinated with the cation (*23*, *24*). The water bridge usually causes a decrease of less than 50 cm^{-1} in the location of the C═O stretching vibration maximum compared to that of the spectrum of the nonadsorbed molecule, while the other type of bond had a stronger effect. The small shift observed for this bond in our study indicates that it may be bound through the hydration water but not through a direct coordination of the cation. This interaction may be related to the acidity of the water molecules in the Wyoming bentonite interlayer (*21*, *25*). Such a low shift of the C═O band due to adsorption by montmoril-

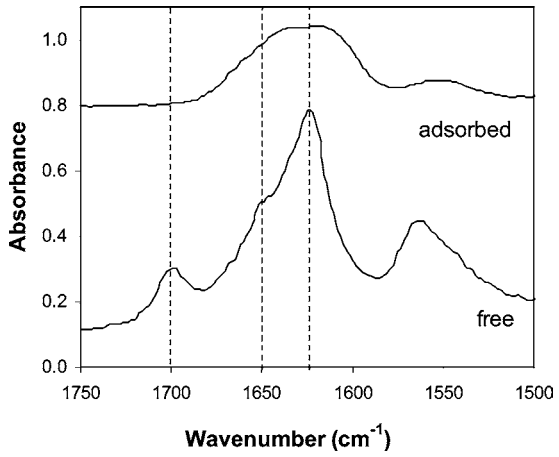

Figure 5. Comparison of the 105 °C treatment effect on free and adsorbed DFOB spectra in the range of 1750–1500 cm^{-1}.

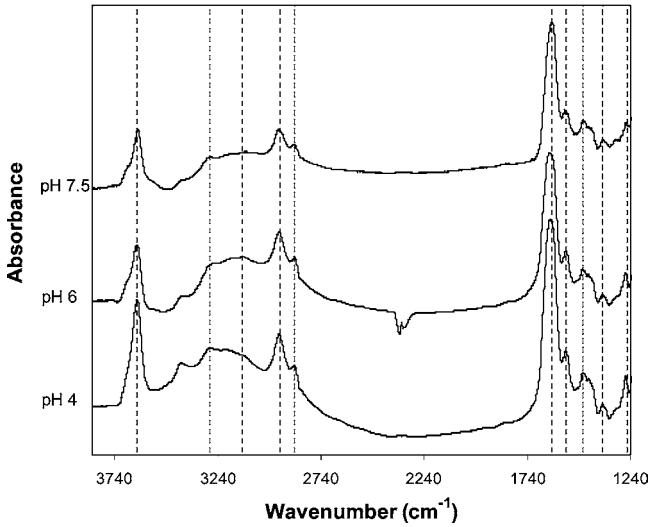

Figure 6. Effects of pH on the infrared spectra of adsorbed DFOB (1 mg, at 25 °C). The spectra are shown in the range 3850–1240 cm^{-1}, after subtraction of the unloaded Ca-montmorillonite spectrum.

lonite was also found for acetamide (*26*), while a reaction of C═O with other smectites was found to be more effective. Earlier studies of amide interactions with montmorillonite reported that, upon dehydration, the C═O formed a direct coordination bond with the cation, reflected by a strong reduction of the carbonyl stretching frequency (*23*, *24*). The appearance of a water band at 1636 cm^{-1} (**Table 1**) suggested that the thermal treatment at 105 °C did not cause a complete dehydration of water molecules from the interlayer, and indeed there was no significant shift in the absorption of C═O after this thermal treatment.

Reduction of the OH stretching frequency toward lower values is typical for adsorbed hydroxyls (*27*, *28*), and it was in most cases attributed to hydrogen bonds with the water molecules of the exchangeable cation. A decrease of 30 cm^{-1} compared to the value for the free sample, which decreased even more following the 105 °C treatment (**Table 1**), implies that intensive hydrogen bonds are involved. The deformation band of OH, observed for the free DFOB at 1397 cm^{-1}, is absent in the spectra of the adsorbed DFOB (**Figure 3b**, **Table 1**). Shifts of the OH deformation band could be toward either lower or higher frequency values following adsorption (*18*). However, no evident new band, which could be attributed to OH deformation, was found in this range (**Table 1**). Still, these observations indicate that a strong involvement of the OH group took place during the adsorption process.

A partial thermal degradation was observed for the free (nonadsorbed) DFOB in the 105 °C treatment, evidently shown by the appearance of a new band at 1700 cm^{-1} (*19*). This phenomenon was not exhibited in the spectra of the adsorbed DFOB under the same conditions (**Figure 5**), implying again the protective effect of the clay. The residual water, which remained in the sample under these conditions (according to the band at 1636 cm^{-1}), may be related to that effect as well. However, upon heating of the samples of the adsorbed DFOB to 170 °C, the conspicuous band of the hydroxamic C═O at 1620 cm^{-1} disappeared, indicating degradation of this group (note differences between the spectrum of adsorbed DFOB at 25 °C, **Figure 3b**, and the spectrum recorded after the 170 °C thermal treatment, **Figure 9**). As a result, the hidden band of the secondary amide at 1650 cm^{-1} was exposed, and became evident in the spectrum of the adsorbed DFOB after the 170 °C thermal treatment (**Figure 9**).

(iii) NH_3^+ *Group*. Due to its high reactivity and the location of characteristic bands of this group (overlapping the absorption bands of the aliphatic groups), the absorption bands of this group are the most difficult to identify in the infrared spectra of DFOB. However, its positive charge and its position at the terminal edge of the pendant tail of the molecule justify special attention for the adsorption process of this group.

New bands appeared in the range of 3250−3170 cm^{-1} following adsorption (**Figure 4**, **Table 1**). This range is related to strongly adsorbed NH_3^+ (*18*); a band at 3236 cm^{-1} is related to a fraction of the NH_3^+ group, which is adsorbed via a water molecule, while the other band at 3192 cm^{-1} can be attributed to NH_3^+ directly adsorbed to the oxygen plane of the montmorillonite (*29*). Indeed, heating the sample to 105 °C affected the former (adsorbed through water molecules), but had no effect on NH_3^+, which was directly bound to the oxygen plane (**Table 1**).

Broad bands at 3032 and 2963 cm^{-1} within the range of the ammonium band in the spectrum of adsorbed DFOB resulted from another fraction of NH_3^+, slightly interacting in the interlayer space. Heating the sample to 105 °C had a strong effect, especially on the symmetric stretching vibration. This effect was not observed with the free DFOB (**Table 1**), indicating that the clay interlayer environment had an influence on this fraction as well. The NH_3^+ deformation band at 1551 cm^{-1} decreased significantly compare to that of the free (nonadsorbed) sample (**Table 1**), indicating the strong interaction of this group in the interlayer space as well. The NH_3^+ group was not disintegrated following the thermal treatment at 170 °C as shown by the persistent shoulder at about 1540 cm^{-1} **(Figure 9)**.

(iv) C−H Interactions. Absorption bands related to CH_3, and even those of CH_2 (which were found to be very stable at various environmental conditions for the free DFOB; *19*), were slightly shifted upon adsorption, and their sharpness was reduced (**Table 1**). Changes in the CH absorption, mainly those of the stretching vibrations (**Table 2**), are related to changes in van der Waals attraction forces (*30*). Remarkable changes in the CH vibrations were found in the range of 1460−1370 cm^{-1} (**Figure 3b** compared to **Figure 3d**, **Table 1**). This is in accordance with the strong interactions of all functional groups of DFOB upon adsorption, since the exact location of the C−H vibration in this range derives from the adjacency of the different functional groups.

(v) pH Effect. The similarity of the spectra at different pH values is in accordance with the stability of the ligand over the

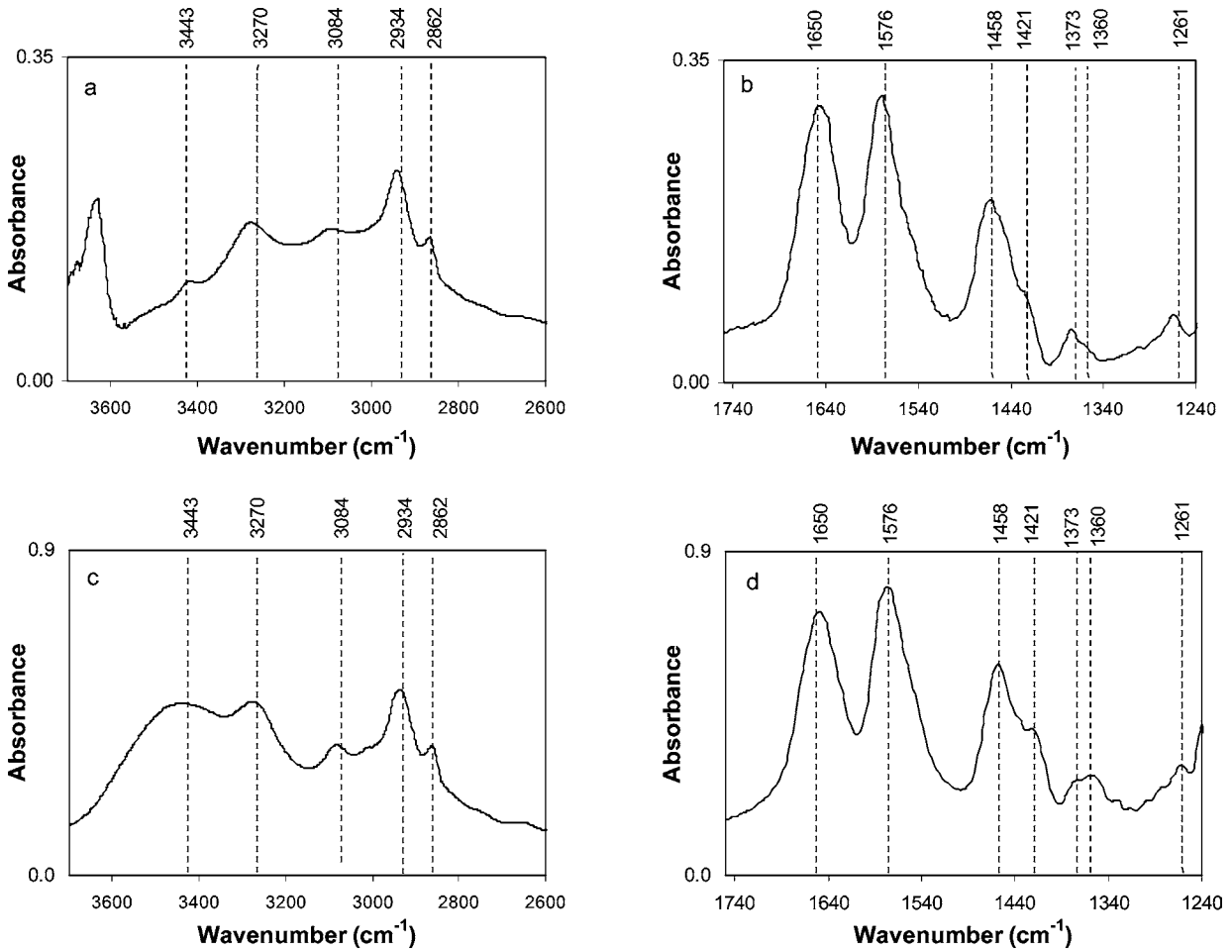

Figure 7. Effects of adsorption on the infrared spectra of FOB (1 mg, 25 °C, pH 7.5), after subtraction of the unloaded Ca-montmorillonite spectrum: (**a**) adsorbed FOB spectrum in the range of 3700–2600 cm^{-1}; (**b**) adsorbed FOB spectrum in the range of 1750–1240 cm^{-1}; (**c**) free FOB spectrum in the range of 3700–2600 cm^{-1}; (**d**) free FOB spectrum in the range of 1750–1240 cm^{-1}.

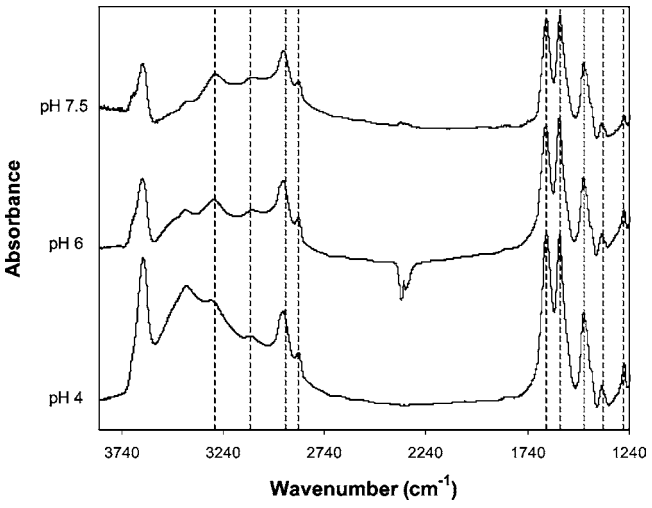

Figure 8. Effects of pH on the infrared spectra of adsorbed FOB (1 mg, at 25 °C). The spectra are shown in the range 3850–1240 cm^{-1}, after subtraction of the unloaded Ca-montmorillonite spectrum.

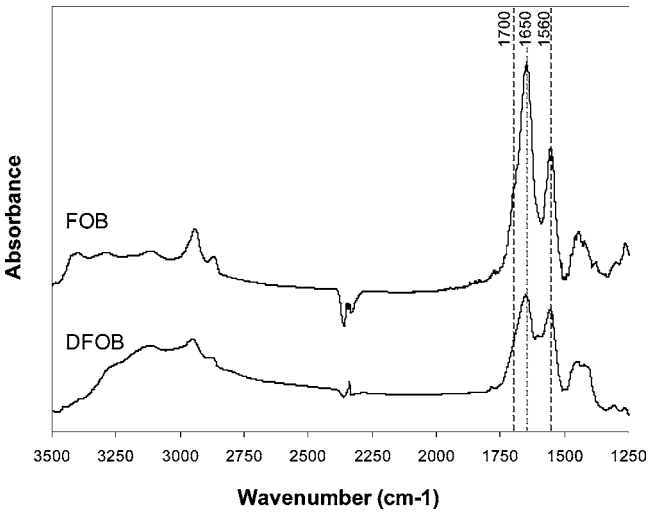

Figure 9. Effect of heating the sample to 170 °C on the spectra of adsorbed DFOB and FOB (1 mg, pH 7.5) in the range 3500–1250 cm^{-1}.

examined pH range. A detailed discussion of this matter was presented in our previous paper (*17*).

Adsorbed FOB. As opposed to those of DFOB, the spectra of FOB changed only slightly following adsorption (**Figure 7**; note the resemblance of the scales, compared to the differences found for DFOB in **Figure 3**).

(i) Secondary Amide Groups. The low frequencies of the stretching bands of the secondary amide group in the free, not adsorbed, FOB were related to specific hydrogen bonds within the Fe complex (*19*). The frequencies of both stretching bands (N−H and C−N−H overtone) of this group increased upon adsorption (**Table 2**), indicating the weakening of intramolecular hydrogen bonds following adsorption into the clay interlayer,

compared to those of the free state. However, the absorption of the C═O bond of this group did not show any surface reaction upon adsorption. The protective effect of the adsorption against thermal degradation of this group at 170 °C appeared here as well, similarly to that of the adsorbed DFOB molecule.

(ii) Hydroxamate Groups. Absorption bands of the groups involved in the Fe complex formation were not changed following adsorption, implying that these groups did not interact with the clay surface. As a result of the thermal treatment at 170 °C, the absorption of the hydroxamic group at around 1576 cm^{-1} disappeared (note differences between the spectrum of adsorbed FOB at 25 °C, **Figure 7d**, and the spectrum recorded after the 170 °C treatment in **Figure 9**), indicating the destruction of the Fe-binding center under these conditions.

(iii) NH_3^+ *Group*. The broad range representing the strongly adsorbed NH_3^+ appeared here in a manner similar to that of DFOB. Bands at 3038 and 2976 cm^{-1} are related to the other fraction of NH_3^+, slightly interacting in the interlayer space. These bands were found in the range of the ammonium band, similarly to those found for adsorbed DFOB. The response of the NH_3^+ group to the heating of adsorbed FOB was more drastic than in the case of adsorbed DFOB. This finding is in accordance with the higher reaction to environmental changes shown by this group in the FOB spectra, compared with that of DFOB (*19*). It was related to a lower interaction with other parts of the somewhat hydrophobic body of the FOB molecule. This group was also found to be relatively resistant to thermal degradation as shown by the shoulder at about 1540 cm^{-1} (**Figure 9**).

(iv) C−H Interactions. The effects of adsorption on CH bending vibrations of FOB were minor compared to those in the analogous range in the DFOB spectrum. Still, bands related to CH_3 and CH_2 were slightly shifted upon adsorption, and their sharpness was reduced (**Table 2**). This finding supports the effect of the interlayer space environment on parts of the FOB molecule (as was mentioned for the N−H of the secondary amide), though the Fe-binding center remained unchanged.

Summary. An earlier study (*19*) dealt with spectral analysis of the free (nonadsorbed) DFOB and of its Fe complex (FOB). In the present study, that interpretation is applied to characterize the adsorption mechanisms of both DFOB and FOB by Ca-montmorillonite. This information is important for the understanding of the siderophore behavior in soils and its potential use as an Fe fertilizer.

No significant effect on adsorption, due to pH changes, was observed at the examined pH range (4−7.5) for both DFOB and FOB. These results are in accordance with our previous batch experiments (*17*). Thermo X-ray diffraction analysis proved penetration of both DFOB and FOB into the interlayer space of Ca-montmorillonite.

Thermo-IR spectroscopy of adsorbed DFOB indicated substantial interaction of all active groups of the organic compounds with active sites on the surface of the clay. These interactions may limit the mobility and function of the free ligand form of the siderophore ferrioxamine B in montmorillonite-rich soils. The strong interaction with OH of the hydroxamic group could potentially reduce Fe binding by the adsorbed ligand.

The FTIR spectrum of FOB, on the other hand, hardly changed as a result of the adsorption. The main interactions of adsorbed FOB with the clay were through the NH_3^+ group and NH of the secondary amide. The hydroxamic groups were not affected by adsorption, implying that the Fe-binding center existed and was not directly influenced by the interlayer space environment. This is in accordance with experiments we conducted on the Fe nutrition of plants reported earlier (*14*), which showed that plants could still use FOB adsorbed by Ca-montmorillonite as an Fe source. However, the cationic tail is assumed to be an important factor in the siderophore uptake systems of microorganisms, due to specific host−guest interaction (*31*, *32*). Therefore, significant adsorption of the NH_3^+ tail of the siderophore in montmorillonite-rich soils could impair the ability of microorganisms to use it as an Fe source. The weakening of intramolecular hydrogen bonds of the secondary amide group, observed upon adsorption of FOB, might induce a change in the stability of its molecular structure, which could also affect its availability to microorganisms and its stability constant with Fe. These aspects need further investigation.

Adsorption mechanisms, observed in addition to cation exchange in this study, explained the significant hysteresis found between adsorption and desorption of the siderophore (*19*). The adsorption by Ca-montmorillonite was found to provide a certain defense against the destructive effect of high temperature on the siderophore. The presence of a proton donor was suggested to prevent that degradation (*19*). Hydration water in the clay interlayer space may play the role of the stabilizing agent. This effect is especially effective in the presence of a metal cation, which polarized the water molecule in its hydration shell, becoming a Bronsted acid. Though the adsorption main mechanism is via cation exchange with the positively charged siderophore (*17*), a significant amount of Ca^{2+} persists as exchangeable cations in these experimental conditions, producing acidic sites in the interlayer. At 170 °C the hydroxamic group, which is essential for the function of the siderophore as a chelating agent, was already completely decomposed, indicating that this group is the most sensitive part of the siderophore to thermal degradation. Interactions which were demonstrated in this study can serve as a model for the prediction of adsorption of other hydroxamate siderophores in soils.

LITERATURE CITED

(1) Chen, Y.; Barak, P. Iron nutrition of plants in calcareous soils. *Adv. Agron*. **1982**, *35*, 217−240.

(2) Chen, Y.; Shenker. M. Agronomic approaches for increasing iron availability to food crops. In Agricultural and molecular genetic approaches to improving nutrition and preventing micronutrient malnutrition globally. In *Encyclopedia of life support systems (EOLSS)*; developed under the auspices of the unesco; Cakmak, I., Graham, R. D., Welch, R. M., Eds.; EOLSS: Oxford, U.K., 2003.

(3) Lindsay, W. L. Iron-oxide solubilization by organic-matter and its effect on iron availability. *Plant Soil* **1991**, *130*, 27−34.

(4) Winkelmann, G. Specificity of iron transport in bacteria and fungi. In *Handbook of microbial iron chelates*; Winkelmann, G., Ed.; CRC Press: Boca Raton, FL, 1991.

(5) Powell, P. E.; Cline, G. R.; Reid, C. P. P.; Szaniszlo, P. J. Occurrence of hydroxamate siderophore iron chelators in soils. *Nature (London)* **1980**, *287*, 833−834.

(6) Powell, P. E.; Szaniszlo, P. J.; Cline, G. R.; Reid, C. P. P. Hydroxamate siderophores in the iron nutrition of plants. *J. Plant Nutr*. **1982**, *5*, 653−673.

(7) Bossier, P.; Verstraete, W. Ecology of arthrobacter jg-9-detectable hydroxmate siderophores in soils. *Soil Biol. Biochem.* **1986**, *18*, 487−492.

(8) Crowley, D. E.; Reid, C. P. P.; Szaniszlo, P. J. Microbial siderophores as iron sorces for plants. In *Iron transport in microbes, plants and animals*; Winkelmann, G., van der Helm, D., Neilands, J. B., Eds.; VCH: Weinheim, Germany, 1987; pp 375−386.

(9) Leong, J.; Raymond, K. N. Coordination isomers of biological iron transport compounds. Iv: Geometrical isomers of chromic desferrioxamine b. *J. Am. Chem. Soc.* **1975**, *97*, 293−296.

(10) Cline, G. R.; Reid, C. P. P.; Powell, P. E.; Szaniszlo, P. J. Effects of hydroxamate siderophore on iron absorption by sunflower and sorghum. *Plant Physiol*. **1984**, *76*, 36−39.
(11) Jurkevitch, E.; Hadar, Y.; Chen. Y. Involvement of bacterial siderophores in the remedy of lime-induced chlorosis in peanut. *Soil Sci. Soc. Am. J.* **1988**, *52*, 1032−1037.
(12) Crowley, D. E.; Wang, Y. C.; Reid, C. P. P.; Szaniszlo, P. J. Mechanisms of iron acquisition from siderophores by microorganisms and plants. *Plant Soil* **1991**, *130*, 179−198.
(13) Wang, Y.; Brown, H. N.; Crowley, D. E.; Szaniszlo, P. J. Evidence for direct utilization of a siderophore, ferrioxamine B, in axenically grown cucumber. *Plant Physiol*. **1993**, *16*, 579−585.
(14) Siebner-Freibach, H.; Hadar, Y.; Chen, Y. Siderophores sorbed on ca-montmorillonite as an iron source for plants. *Plant Soil* **2003**, *251*, 115−124.
(15) Martell, A. E.; Smith, R. M.; Motekaitis, R. J. NIST Critically selected stability constants of metal complexes database (v. 4), Standard Reference Data Program, Gaithersburg, MD, 1997.
(16) Dhungana, S.; White, P. S.; Crumbliss, A. L. Crystal structure of ferrioxamine b: A comparative analysis and implications for molecular recognition. *J. Biol. Inorg. Chem.* **2001**, *6*, 810−818.
(17) Siebner-Freibach, H.; Hadar, Y.; Chen, Y. Interaction of iron chelating agents with clay minerals. *Soil Sci. Soc. Am. J.* **2004**, *68*, 470−480.
(18) Yariv, S. Ir spectroscopy and thermo-ir spectroscopy in the study of the fine structure of organo-clay complexes. In *Organo-clay complexes and interactions*; Yariv, S., Cross, H., Eds.; Marcel Dekker: New York, 2002.
(19) Siebner-Freibach, H.; Yariv, S.; Lapides, Y.; Hadar, Y.; Chen, Y. Thermo-Ftir spectroscopic study of the siderophore ferrioxamine B: spectra analysis and stereochemical implications of iron chelation, pH and temperature. *J. Agric. Food Chem.* **2005**, *53*, 3434−3443.
(20) Yariv, S.; Lapides, I. The use of thermo-XRD-analysis in the study of organo-smectite complexes. Robert Mackenzie memorial lecture. *J. Therm. Anal. Calorim.* **2005**, *80*, 11−26.
(21) Yariv, S. Wettability of clay minerals. In *Modern approaches to wettability*; Schrader, M. E., Loeb, G., Eds.; Plenum Press: New York, 1992; pp 279−326.
(22) Nasser, A.; Gal, M.; Gerstl, Z.; Mingelgrin, U.; Yariv, S. Adsorption of alachlor by montmorillonites. *J. Therm. Anal.* **1997**, *50*, 257−268.
(23) Tahoum, S. A.; Mortland, M. M. Complexes of montmorillonite with primary, secondary and tertiary amides. I. Protonation of amides on the surface of montmorillonite. *Soil Sci.* **1966**, *102*, 248−254.
(24) Tahoum, S. A.; Mortland, M. M. Complexes of montmorillonite with primary, secondary and tertiary amides. Ii. Coordination of amides on the surface of montmorillonite. *Soil Sci*. **1966**, *102*, 314−321.
(25) Yariv, S. The effect of tetrahedral substitution of si by al on the surface acidity of the oxygen plane of clay minerals. *Int. Rev. Phys. Chem*. **1992**, *11*, 345−375.
(26) Ogawa, M.; Nagafusa, Y.; Kuroda, K.; Kato, C. Solid-state interaction of acrylamide into smectites and na-taeniolite. *Appl. Clay Sci*. **1992**, *7*, 291−302.
(27) Fenn, D. B.; Mortland, M. M. Interlamellar metal complexes in the layer silicates. II. Phenol complexes in smectites. In *Proceedings of the International Clay Conference*, Madrid, Spain, 1972; Serratosa, J. M., Ed.; Divsion de ciencias C.S.I.C.: Madrid, Spain, 1973; pp 591−603.
(28) Breen, C.; Flynn, J. J.; Parkes, G. M. B. Thermogravimetric, infrared and mass-spectroscopic analysis of the desorption of methanol, propan-1-ol, propan-2-ol and 2-methylpropan-2-ol from montmorillonite. *Clay Miner*. **1993**, *28*, 123−137.
(29) Yariv, S.; Heller, L. Sorption of cyclohexylamine by montmorillonite. *Isr. J. Chem*. **1970**, *8*, 935−945.
(30) Fripiat, J. J.; Pennequin, M.; Poncelet, G.; Cloos, P. Influence of the van der Waals forces on the infrared spectra of short aliphatic alkylammonium cations held on montmorillonite. *Clay Miner*. **1969**, *8*, 119−134.
(31) Spasojevic, I.; Crumbliss, A. L. Bulk liquid membrane transport of ferrioxamine b by neutral and ionizable carriers. *J. Chem. Soc., Dalton Trans*. **1998**, *23*, 4021−4027.
(32) Ziv, C. Characterization of structure−function relationship of iron uptake by microorganisms: The use of biomimetric synthetic analogs of ferrioxamine B. M.A. Thesis, Faculty of Agriculture, The Hebrew University of Jerusalem, Rehovot, Israel, 2000.

Received for review August 7, 2005. Revised manuscript received November 16, 2005. Accepted December 2, 2005.

JF051924E